Quantitative In Situ Monitoring of Parahydrogen Fraction Using Raman Spectroscopy

Andrew J. Parrott[1] , Paul Dallin[2], John Andrews[2],
Peter M. Richardson[3] , Olga Semenova[3] , Meghan E. Halse[3] ,
Simon B. Duckett[3], and Alison Nordon[1]

Abstract

Raman spectroscopy has been used to provide a rapid, noninvasive, and nondestructive quantification method for determining the parahydrogen fraction of hydrogen gas. The basis of the method is the measurement of the ratio of the first two rotational bands of hydrogen at $355\,cm^{-1}$ and $586\,cm^{-1}$ corresponding to parahydrogen and orthohydrogen, respectively. The method has been used to determine the parahydrogen content during a production process and a reaction. In the first example, the performance of an in-house liquid nitrogen cooled parahydrogen generator was monitored both at-line and on-line. The Raman measurements showed that it took several hours for the generator to reach steady state and, hence, for maximum parahydrogen production (50%) to be reached. The results obtained using Raman spectroscopy were compared to those obtained by at-line low-field nuclear magnetic resonance (NMR) spectroscopy. While the results were in good agreement, Raman analysis has several advantages over NMR for this application. The Raman method does not require a reference sample, as both spin isomers (ortho and para) of hydrogen can be directly detected, which simplifies the procedure and eliminates some sources of error. In the second example, the method was used to monitor the fast conversion of parahydrogen to orthohydrogen in situ. Here the ability to acquire Raman spectra every 30 s enabled a conversion process with a rate constant of $27.4 \times 10^{-4}\,s^{-1}$ to be monitored. The Raman method described here represents an improvement on previously reported work, in that it can be easily applied on-line and is approximately 500 times faster. This offers the potential of an industrially compatible method for determining parahydrogen content in applications that require the storage and usage of hydrogen.

Introduction

Molecular hydrogen (H_2) exists as two nuclear spin isomers: the anti-symmetric singlet nuclear spin state parahydrogen (pH_2) and the symmetric triplet spin nuclear state orthohydrogen (oH_2). The equilibrium distribution of the two isomers is a function of temperature. At room temperature, the equilibrium composition is approximately 25% pH_2 and 75% oH_2, a mixture typically referred to as normal hydrogen (nH_2). At lower temperatures the equilibrium distribution shifts to favor the lower-energy pH_2 isomer, so that at its boiling point (20.3 K) the equilibrium composition of H_2 is almost 100% pH_2. However, as the conversion between oH_2 and pH_2 is forbidden, conversion between isomers is very slow unless a catalyst is used.[1–5]

The pH_2 isomer is useful for a wide range of applications, including: liquid fuels;[6–8] matrix isolation spectroscopy;[9,10] certain hyperpolarization methods for nuclear magnetic resonance (NMR) spectroscopy;[4,3,11,12] and as a moderator for spallation neutron sources.[13,14] For many of these

[1]WestCHEM, Department of Pure and Applied Chemistry and CPACT, University of Strathclyde, Glasgow, UK
[2]Clairet Scientific Ltd., Northampton, UK
[3]Centre for Hyperpolarisation in Magnetic Resonance (CHyM), Department of Chemistry, University of York, York, UK

Corresponding author:
Alison Nordon, WestCHEM, Department of Pure and Applied Chemistry and CPACT, University of Strathclyde, Glasgow, UK.
Email: alison.nordon@strath.ac.uk

applications, the proportion of the pH_2 isomer is of vital importance. For example, for fuel applications H_2 is usually stored as a liquid. If the oH_2 is not fully converted to pH_2 (e.g., by passing over a suitable catalyst) before condensation from the gas state, then the slow exothermic conversion of oH_2 to pH_2 will liberate enough heat to vaporize up to 64% of the liquid.[7] For pH_2-based hyperpolarization methods in NMR, the greater the level of pH_2 enrichment, the greater the NMR signal enhancement.[4,11,15] Indeed various methods of generating high purity pH_2 for NMR studies have been reported[15,16] and major NMR vendors also supply this type of specialized equipment.[17]

The research group at the University of Strathclyde has an in-house built pH_2 generator, which is used to provide gaseous pH_2 for signal amplification by reversible exchange (SABRE) hyperpolarization studies on a bench-top NMR spectrometer.[18–20] To validate the hyperpolarization experiments, it is desirable to be able to rapidly monitor the pH_2 fraction produced by this generator. The two spin isomers differ slightly in several physical properties, such as: heat capacity, vapor pressure, speed of sound, and thermal conductivity. These properties can be used to measure the pH_2 enrichment in an unknown sample.[4,9,21–23] Nevertheless, many of these measurements often require that other parameters also be measured very accurately (e.g., temperature and pressure) and require calibration with known mixtures to provide quantitative results.[15,21,24] However, as the two spin isomers occupy different rotational energy levels,[1,3,4,25] it is possible to use Raman spectroscopy to probe the rotational transitions of H_2 gas and hence determine the composition of pH_2 without calibration mixtures.[8,13,14,25,26]

In the context of monitoring pH_2 enrichment, Sundararajan et al.[10] used a Raman microscope with a 514 nm laser for off-line monitoring of H_2 gas used for matrix isolation spectroscopy. They reported that even with 1000 scans, the analysis could not be conducted quantitatively. Teshigawara et al.[14] used a Raman microscope for off-line monitoring of H_2 moderators in a neutron source. They did not report the analysis time but did claim that sufficient signal was obtained for quantitative analysis. Matthews et al.[8,26] reported the use of a specialized gas cell for off-line monitoring of H_2 gas from a liquid hydrogen storage tank. They used a 532 nm laser and reported an integration time of only 60 s. However, the density of the gas measured (and hence pressure) was much higher (12 g L^{-1}) than typically produced by the pH_2 generator used here (0.5 g L^{-1}). Sutherland et al.[13] reported an on-line method using a fiber optic coupled probe to monitor the pH_2 fraction in a H_2 moderator used for a neutron source. However, they reported relatively long analysis times of around 20 min per measurement.

Here we report that by using a Raman spectrometer fitted with a non-contact optic, with a backscattering 180° geometry, the acquisition of Raman spectra of H_2 gas from the in-house built pH_2 generator can be greatly simplified. This allows Raman spectra from at-line samples to be easily acquired using existing infrastructure (i.e., conventional NMR tubes). Also, this configuration allows the facile set-up of an on-line method of monitoring the performance of the generator, by focusing the laser onto a simple glass flow tube in the flow path of the generator. The rapid nature of the Raman procedure (every 30 s) enables in situ monitoring of the fast back conversion of pH_2 to oH_2 inside contaminated NMR tubes.

Experimental

At-line and on-line Raman analysis was used to characterize an in-house built pH_2 generator, the schematic of which is shown in Fig. 1. nH_2 gas with a room temperature equilibrium content of pH_2 was produced from water using a hydrogen generator (HG) electrolysis cell (Peak Scientific), operating at 4 bar for at-line experiments and 5 bar for on-line experiments. The nH_2 gas then flowed into a two-way valve (V1), which directed the gas into either a chamber for enrichment of the pH_2 content or directly into the rest of the system. The chamber for the enrichment of pH_2 content was of similar design to that reported previously in the literature.[4,27] Briefly, it consisted of a copper coil (C) (OD = 9.5 mm, ID = 7.7 mm, L = 3 m) packed with charcoal (Sigma-Aldrich), which was submerged in a Dewar (D) filled with liquid nitrogen. The charcoal was held in place with two 40 μm in-line filters (F) at either end of the coil. On-off valves (V2, V3, V4) were used to control whether nH_2- or pH_2-enriched gas was provided to the outlet of V4. The system was equipped with a pressure transducer (P) (Omega) to check the pressure of the gas as well as a vacuum pump (V) (Vacuubrand, ultimate vacuum of 7 mbar) to allow the system (and any connected flow tube (FT) or NMR tube) to be evacuated of gas.

At the start of each experiment, the copper coil was filled with H_2 to the desired pressure without being cooled. The coil was then purged so that the pressure was just above atmospheric and filled again to ensure that only H_2 gas was entering the system. The coil was then cooled with liquid nitrogen and the purge process repeated. Once the pressure in the coil had again reached the desired level (usually after around 15 min), this was regarded as the start of the generator running time.

For at-line Raman analysis, the outlet of V4 was connected to a standard NMR tube (Wilmad Precision, 527-PP-7) equipped with a Young's valve (GPE Scientific) (not shown in Fig. 1). For on-line analysis, V4 was connected to a FT which had a 40 mm section of the same type of NMR tube partway along its length. The outlet of the FT was connected to a pneumatic control unit (Bruker) for a polarizer box (PB) (as shown in Fig. 1), which controlled when gas flowed along the FT into the PB and then out into the atmosphere. The PB was used to allow gas to
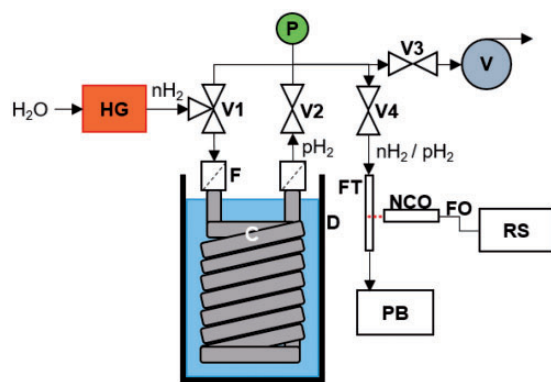
Figure 1. Schematic of the in-house built pH_2 generator. H_2 gas at 4 bar for at-line experiments, or 5 bar for on-line experiments (as shown in figure), was produced from water using a hydrogen generator (HG) electrolysis cell. The gas flowed into a two-way valve (V1), which directed the gas into either a chamber for enrichment of the pH_2 content or directly into the rest of the system. The chamber for the enrichment of pH_2 content is a copper coil (C) (OD = 9.5 mm, ID = 7.7 mm, L = 3 m) packed with charcoal, which was submerged in a Dewar (D) filled with liquid nitrogen. The charcoal was held in place with two 40 μm in-line filters (F) at either end of the coil. On-off valves (V2, V3, V4) were used to control whether nH_2- or pH_2-enriched gas was provided to the outlet of V4. The system pressure was measured using a pressure transducer (P). A vacuum pump (V) was used to allow the system (and any connected flow tube (FT) or NMR tube) to be evacuated of gas.

flow for 15 s, with a desired interval (typically around every 5 min) between each flow duration. Between intervals, the PB held the gas pressure constant at 5 bar in the FT. The PB has previously been used to automate SABRE NMR experiments,[19,20,28,29] but in this case it was simply used to control the flow of gas out of the pH_2 generator.

The Raman spectrometer (RS) used to record the spectra of the gas samples was a RamanRxn1 analyzer (Kaiser Optical Systems), which utilized a CW diode laser with a maximum output of 400 mW at 785 nm. The axial transmissive spectrograph (f/1.8) was equipped with a holographic transmission grating (HoloPlex). The detector was a charged coupled device cooled to −40 °C (Peltier cooling). The spectral range was 100–3425 cm^{-1} (Raman shift) with an average spectral resolution of 4 cm^{-1}. The spectrometer was coupled with a 5 m fiber optic (FO) cable to a filtered MR probe fitted with a non-contact optic (NCO). This NCO was used to focus the laser onto the center of the NMR tube for at-line or in-situ analysis, or the center of the NMR tube section within the FT for on-line analysis. The same optic was used to collect the backscattered light (180° geometry) from the sample. The NCO had a 10 mm focal length and the size of the focused beam was approximately 100 μm at the focal point. The laser power was around 270 mW at the sample. The spectrometer was

calibrated with a neon atomic line source and a NIST traceable white light source for wavelength and intensity accuracy, respectively. The calibration was verified using a cyclohexane standard before any analysis. A single scan with an integration time of 25 s was used for each spectrum. A dark spectrum, also of 25 s, was recorded before each scan and used for dark correction, giving a total acquisition time of around 50 s. For the experiments studying the stability of pH_2 in an NMR tube using a sampling frequency of 30 s, a single dark spectrum was recorded just before presenting the tube to the laser and used to correct all of the recorded spectra for that sample.

Immediately after recording the at-line Raman spectrum of H_2 contained in a standard NMR tube, the ^1H NMR spectrum was also recorded in a method similar to that reported previously.[15,16,21,27] The sample was placed in a bench-top NMR spectrometer (Magritek Spinsolve) operating at a ^1H Larmor frequency of 43.5 MHz. A spectrum was recorded using a standard 90° pulse and detect sequence, with a bandwidth of 200 kHz, and 512 points per free induction decay (acquisition time of 2.56 ms) zero filled to 2048 points. A repetition time of 300 ms was used between scans. This duration is sufficiently larger than the T_1 of oH_2, which is reported as being in the range of 3–15 ms,[27] to allow for quantitative analysis. A total of 256 scans were acquired, resulting in a total acquisition time of 77 s.

All data analysis was conducted in the R programming environment.[30] The hyperSpec package[31] was used to load the Raman data, and the robust baseline correction algorithm provided by the baseline package[32] (with a span setting of 0.1) was used to remove the influence of the glass background in the Raman spectra.

Results and Discussion

Raman Spectra of Hydrogen Gas

Gas analysis by Raman spectroscopy can be challenging, because the small scattering cross-sections and low densities of the molecules in the gas phase lead to weak Raman signals.[33–35] Therefore, to confirm if sufficient signal could be obtained using our Raman set up, the spectra from an evacuated NMR tube ($\approx$ 7 mbar), a tube filled to 4 bar with H_2 gas directly from the hydrogen generator (i.e., nH_2), and a tube filled to 4 bar from the pH_2 generator after it had been running for 2 h were compared. The resulting spectra are shown in Fig. 2. From this figure, it can be seen that peaks for the first two rotational bands of hydrogen at the expected Raman shifts of 355 cm^{-1} and 586 cm^{-1} are clearly visible in the spectra of the two gas samples. These correspond to the rotational transitions $S_0(0)$ ($J = 0 \rightarrow 2$) and $S_0(1)$ ($J = 1 \rightarrow 3$). Two further much weaker bands at 812 cm^{-1} and 1032 cm^{-1} were also observed (see Fig. S1 in the Supplemental Material),
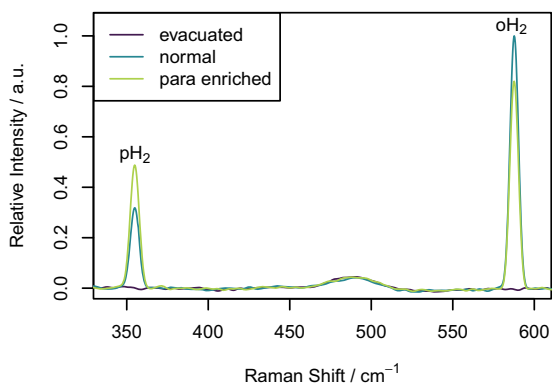
Figure 2. Raman spectra of an evacuated NMR tube, a tube filled with nH_2 at 4 bar, and a tube filled with pH_2-enriched H_2 at 4 bar.

corresponding to the transitions $S_0(2)$ $(J = 2 \rightarrow 4)$ and $S_0(3)$ $(J = 3 \rightarrow 5)$ respectively.[25,36] Higher rotational levels were not observed because these levels are not significantly populated at room temperature.[3,36] From the spectrum of the evacuated tube, it can be seen that sampling through the glass wall of the NMR tube does not complicate the spectrum in this region, except with a broad glass signal which can be easily removed with baseline correction (see Fig. S1 for examples of non-baseline correct spectra). As expected, the spectrum from the pH_2-enriched sample had a much greater proportion of signal from the rotational band corresponding to the pH_2 isomer, compared to the spectrum from the nH_2 sample.

As pH_2 and oH_2 isomers occupy different rotational energy levels, with pH_2 occupying even values of J (0, 2,...) and oH_2 occupying odd values of J (1, 3,...),[1,3,4,37] the ratio of these bands can be used to determine the para : ortho ratio.[25] Here we used the same calculation method as reported by Matthews et al.[8,26] Briefly, the Raman scattering intensities, I_J, of the rotational bands of H_2 are given by Eq. 1

$$I_J = \frac{(J+1)(J+2)}{(2J+1)(2J+3)} x_J p_J \gamma_J^2 \omega_s^3 \qquad (1)$$

where x_J is the fraction of gas at the Jth level, p_J is the Boltzmann population of the Jth level at the measurement temperature, γ_J is the anisotropy of the polarizability tensor, and ω_s is the scattered light angular frequency. Therefore, the ratio of the areas of the first two rotational bands (I_0 and I_1 at 355 cm^{-1} and 586 cm^{-1}, respectively) can be used to calculate the ratio of x_0 and x_1, and hence the para : ortho ratio, r, as shown by Eq. 2.

$$r = \frac{x_0}{x_1} = \frac{3 I_0 p_1 \gamma_1^2}{5 I_1 p_0 \gamma_0^2} \qquad (2)$$

This can be simply rearranged to give the pH_2 fraction, x_{pH_2}, as shown by Eq. 3.

$$x_{pH_2} = \frac{r}{1+r} \qquad (3)$$

p_J must be considered, as not all pH_2 molecules will occupy the $J = 0$ ground rotational energy level (likewise not all oH_2 molecules will occupy $J = 1$) at the measurement temperature (294 K).[1,3,37] Values for p_J were calculated using Boltzmann's distribution law,[1,3] with a rotational temperature of hydrogen, θ_R, of 87.6 K.[3,38] The values reported by Hunt et al.[39] were used for γ_J.

Using this method, x_{pH_2} for the Raman spectrum of the nH_2 sample shown in Fig. 2 was calculated as being 25.6%. This value is very close to the expected equilibrium value of 25.1% for H_2 at 294 K. Equilibrium values of x_{pH_2} can be calculated using Boltzmann statistics.[1,3,11] For the pH_2-enriched sample, x_{pH_2} was calculated as being 39.5%. While this shows some enrichment over the nH_2 sample, the enrichment is much lower than the 52.1% expected at the 77 K operating temperature of the pH_2 generator. This discrepancy could be due to the generator requiring > 2 h to reach its maximum x_{pH_2} output, or because conversion of pH_2 back to oH_2 is occurring inside the NMR tube. These two issues are explored below.

At-Line and On-Line Monitoring of Generator Performance

Normally it is assumed that when H_2 gas is passed over a catalyst, such as the charcoal used here, the thermodynamic equilibrium position is obtained rapidly, usually within a few minutes.[4,11,40] However, as discussed above, it appears that the generator used here requires considerably longer to reach the equilibrium x_{pH_2} at its operating temperature. To investigate how long the pH_2 generator takes to reach steady state, a series of at-line samples of H_2 gas were taken for Raman analysis over an 8 h time period. The analysis was repeated on several different days to check for consistency of performance. The results are presented in Fig. 3, which shows that the pH_2 fraction gradually increases from around 32% to around 43.5% within 2 h. After 2 h, the increase in x_{pH_2} begins to flatten out, and it takes > 8 h before a fairly steady production of around 50% is achieved. From Fig. 3 it can also be seen that the generator performs similarly over several different days of operation, with some scatter caused possibly by different operating conditions in the laboratory (e.g., the room temperature which will affect the temperature of the H_2 gas entering the conversion chamber). The data from each separate day of operation can be fitted to the exponential function given in Eq. 4,

$$x_{pH_2}(t) = \left[x_{pH_2}(0) - x_{pH_2}^f \right] \exp\left(\frac{-t}{\tau}\right) + x_{pH_2}^f \qquad (4)$$
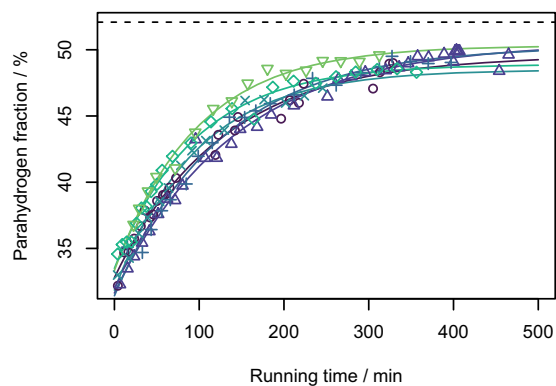
Figure 3. Plots of parahydrogen fraction (x_{pH_2}) against generator running time for experiments conducted on six different days (different symbol shapes and colors). Samples were taken for Raman analysis by filling NMR tubes with pH$_2$-enriched H$_2$ at 4 bar. The black horizontal dashed line shows the equilibrium value x_{pH_2} at the generator operating temperature (77 K). The solid lines show the fits of the data points from each day to the exponential function Eq. 4 (details in the main text and Table SI).

Figure 4. Plots of x_{pH_2} against time for the in-house built pH$_2$ generator. x_{pH_2} was calculated from on-line Raman measurements of the gas flowing at 5 bar between the generator and a pneumatic control unit. Raman spectra were recorded every 60 s. The control unit was set to take 15 s samples of H$_2$ every 340 s before point A, every 160 s between points A and B, every 100 s between points B and C, and every 220 s after point C. The solid line is a local polynomial regression (loess) fitting through the data, calculated using a span of 0.2.

where $x_{pH_2}(t)$ is the pH$_2$ fraction at time t, $x_{pH_2}(0)$ is the pH$_2$ fraction at time zero, τ is a time constant, and $x_{pH_2}^{f}$ is the final pH$_2$ fraction as time approaches infinity. Values in the ranges of 94–142 min, 31.4–33.5%, and 48.5–50.5% were estimated for τ, $x_{pH_2}(0)$, and $x_{pH_2}^{f}$ respectively, using non-linear least squares regression (see Table SI for full details). One possible reason why $x_{pH_2}^{f}$ does not reach the equilibrium value of 52.1% expected for pH$_2$ fraction at liquid nitrogen temperatures is that the gas flowing through the coil does not reach 77 K due to insufficient cooling. A value of 50.0% for $x_{pH_2}^{f}$ instead suggests a slighter higher temperature of 80 K.

Gamliel et al.[27] also used a liquid nitrogen cooled pH$_2$ generator (although with an iron(III) oxide catalyst), and used NMR spectroscopy to measure x_{pH_2} of the resulting enriched gas. They reported a slow increase in x_{pH_2} over time, with 42.3% reached after around 2 h, increasing to 46.3% after 3.7 h. This is broadly similar to the rate of increase shown in Fig. 3. They also report that the increase in x_{pH_2} is not linear with time, although they do not specify the form of the non-linear behavior.

To monitor the performance of the pH$_2$ generator on-line, a simple glass tube was inserted between the outlet of the generator and the inlet of a pneumatic control unit, as shown in Fig. 1. This control unit is normally used to control the input of pH$_2$ into a mixing chamber used for hyperpolarization experiments.[19,20,28] In this case the pneumatic control was used to regulate the pressure in the flow tube and to control the flow of gas out of the pH$_2$ generator. The Raman laser was focused onto the inside of the glass tube to provide in-situ analysis of the composition of the H$_2$ gas flowing directly out of the generator and into the control unit.

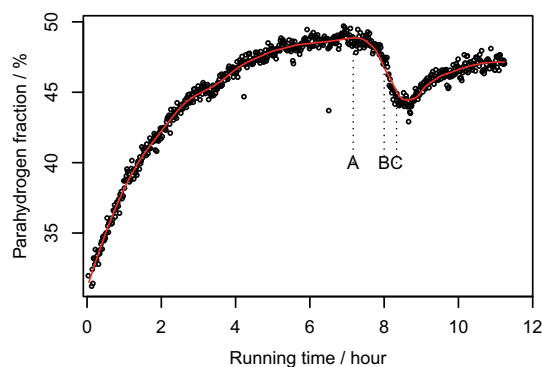Figure 4 shows the result of the calculated values of x_{pH_2} from the on-line Raman monitoring of the generator output. For the first 7 h of running time (before point A on Fig. 4), the pneumatic control unit was set to sample H$_2$ every 340 s. A sample by the pneumatic control unit consisted of a flow of gas regulated down from 5 bar to 4 bar for 15 s. As can be seen from Fig. 4, x_{pH_2} increases from around 30% to 40% within the first 4 h, and a further 2 h is then required to reach 48%. This trend is similar to the case when at-line sampling was used (see Fig. 3).

The sampling frequency used in hyperpolarization studies that also use a similar pneumatic control unit is reported as being in the range of 10–45 s,[20,28,41] which is much more rapid than the once per 340 s used here. Therefore, after reaching steady state, the performance of the pH$_2$ generator was tested by increasing the sampling frequency of the pneumatic control unit to once every 160 s (between points A and B on Fig. 4) and then to once every 100 s (between points B and C on Fig. 4). From Fig. 4, it can be seen that x_{pH_2} decreases rapidly after point A. After point C, the sampling frequency was reduced to once every 220 s; after this point, x_{pH_2} gradually increases again back towards the maximum value of x_{pH_2}. As the pneumatic control unit regulates when flow occurs within the pH$_2$ generator, a quicker sampling frequency results in a shorter residence time for the gas within the coil that contains the conversion catalyst, and hence less contact time for conversion from oH$_2$ into pH$_2$. This explains why the x_{pH_2} decreases when the sampling frequency is too fast.

These results clearly show that the generator used here would not be suitable for use with very high sampling frequencies, as the x_{pH_2} would fluctuate depending on the resulting residence time. This important observation may have been missed without the use of rapid on-line

monitoring. On-line monitoring could be used to judge the performance of any improved designs for the pH_2 generator to make sure that performance is optimized and consistent. Possible improvements include: using various other catalyst materials such as hydrous ferric oxide[37] instead of charcoal; increasing the submerged coil volume so that the residence time of the gas within the conversion chamber is increased; and increasing the surface area for heat transfer between the liquid nitrogen and the H_2 gas on the surface of the catalyst.

Comparison and Validation with Nuclear Magnetic Resonance Measurements

To validate the Raman measurements, NMR analysis was also conducted on the pH_2-enriched gas provided from the generator. As the samples taken for the at-line study with Raman were in standard NMR tubes, the exact same samples could be used for NMR analysis by simply inserting the sample into the bore of the NMR instrument. Here we used a bench-top NMR instrument (^1H frequency of 43.5 MHz). While this provided less signal intensity than a high field instrument, it allowed the analysis to be conducted at-line, i.e., the pH_2 generator, Raman spectrometer, and NMR spectrometer were all located within the same laboratory.

Quantification of x_{pH_2} in the gas phase by NMR can be challenging because of the low density of spins (e.g., compared to the liquid phase) and because pH_2 is NMR silent.[16] However, the ortho isomer is NMR visible and the x_{pH_2} can be calculated by taking the ratio of peak area from an unknown sample to that of a known sample (at the same gas density), usually nH_2.[15,16,21,27] Therefore, the NMR method only requires a single reference sample and no further calibration is needed.

Figure 5 compares the NMR spectra of a tube filled with nH_2- and pH_2-enriched H_2 at 4 bar. As expected, the signal is very broad[16,27] (around 100 ppm or 4350 Hz) and the area is lower for pH_2-enriched gas. As can also be seen from the spectra of an evacuated NMR tube in Fig. 5, there is a significant background signal. To correct for this, the background signal was subtracted from the spectra of the nH_2 samples and the at-line samples (see Fig. S2 for example corrected spectra) in a similar method to that reported by Hövener et al.[16]

x_{pH_2} was calculated from the at-line NMR spectra of H_2 gas in the NMR tubes using Eq. 5.[15]

$$x_{pH_2} = 1 - x_{oH_2} \frac{S_0}{S_{ref}} \qquad (5)$$

where S_0 is the area of the oH_2 peak in the NMR spectrum of an unknown sample and S_{ref} is the area of the oH_2 peak in the NMR spectrum of a sample with a known oH_2 composition x_{oH_2}. An NMR tube filled with H_2 directly from the
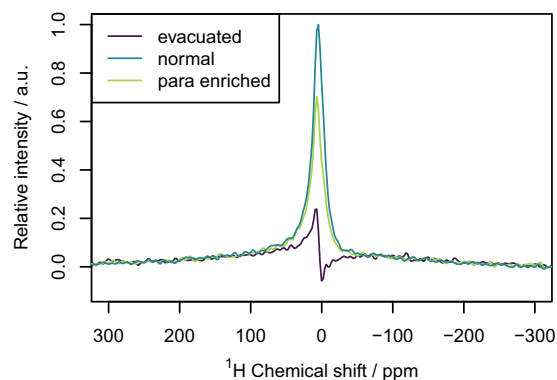

Figure 5. Nuclear magnetic resonance spectra of an evacuated NMR tube, a tube filled with nH_2 at 4 bar, and a tube filled with pH_2-enriched H_2 at 4 bar.

hydrogen generator at 4 bar and 294 K was used as the reference sample. The tube was filled and measured five times to account for slight deviations in filling pressure and the average area was used as the value for S_{ref}. Based on the measurement temperature, x_{oH_2} was calculated as 74.9%. Figure 6 shows the comparison of x_{pH_2} calculated from at-line samples using Raman and NMR analysis; it can be seen that there is very good agreement between the two methods, with $R^2 = 0.991$ and RMSE $= 0.48\%$.

Although there is excellent agreement between the two measuring techniques, Raman analysis has several advantages over NMR for this application. The Raman technique does not require a reference sample, as both spin isomers can be directly detected, which simplifies the procedure and eliminates some sources of error. In NMR analysis, pH_2 is only measured indirectly by measuring the change in the oH_2 signal. While accurate results can be achieved with the pH_2 fractions analyzed from the generator used in this work ($x_{pH_2} < 52\%$), it would be more difficult to analyze higher pH_2 fractions from a more efficiently cooled generator. This is because there is less oH_2 signal to measure with NMR as the pH_2 fraction increases. As NMR is an indirect method, it therefore requires a reference sample with a known composition of oH_2. An obvious choice is to use another tube filled with hydrogen that has a room temperature equilibrium composition of oH_2 (i.e., nH_2). Although this assumes that the reference and unknown samples are filled to the same density, i.e., the same temperature and pressure.[15,21] To avoid this problem, Feng et al.[15] also used the unknown sample as the reference sample, by waiting 72 h for the sample to return to the room temperature equilibrium composition of oH_2. However, this assumes no leaking of the sample and the method is not compatible with taking multiple samples in quick succession. Therefore, we used the approach of using a separate sample of nH_2 as the reference, as used elsewhere.[16,21,27]
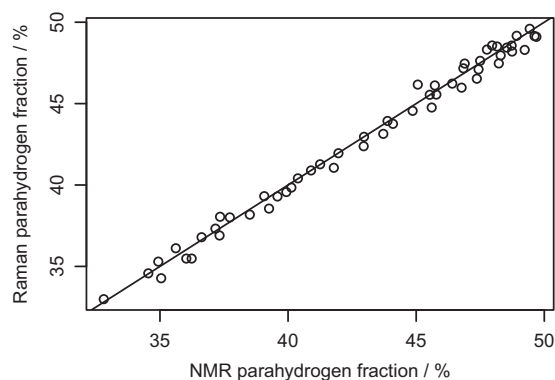
Figure 6. Plot of x_{pH_2} calculated using the Raman spectra, against x_{pH_2} calculated using the NMR spectra from the same at-line samples. The solid line shows the $y = x$ line.

The temperature of the laboratory was measured with a standard kerosene-in-glass thermometer with an accuracy of ± 1.5 K, and the pressure of the gas in the tube was measured with a pressure transducer with an accuracy of ± 0.008 bar. Taking into account the density of H_2,[42] this added an uncertainty of $\pm 1.1\%$ to the values of x_{pH_2} measured by NMR. As the at-line samples were filled manually, the repeatability of pressure was only better than ± 0.05 bar between different samples. This resulted in an uncertainty of $\pm 2.6\%$ to the values of x_{pH_2} (see Fig. S3 for details). The Raman method is insensitive to changes in density between samples, because this changes the intensity of the peaks but not the ratio between the peaks. Therefore, an accurate result could be obtained as long as the filling density was high enough to provide sufficient signal.

Both the Raman and the NMR methods require calculation of the Boltzmann distribution between rotational energy levels of H_2, to calculate p_0 and p_1 in Eq. 2 for Raman, and to calculate x_{oH_2} in Eq. 5 for NMR. These calculations required the temperature of the gas to be measured. However, as the Boltzmann distribution only varies slowly around room temperature, this added an uncertainty of less than $\pm 0.1\%$ for Raman analysis and $\pm 0.01\%$ for NMR analysis (see Figs S4 and S5 for details).

In Situ Monitoring of the Conversion of pH_2 in Nuclear Magnetic Resonance Tubes

Conversion between oH_2 and pH_2 spin isomers is forbidden, so spontaneous gas phase conversion is very slow.[3,5,37] However, the glass wall of an NMR tube (e.g., as used for a SABRE hyperpolarization experiment) offers a surface for the heterogeneous conversion between spin isomers, which is more rapid.[15,37] Various paramagnetic species in the glass wall (or in the sample) may also accelerate the conversion.[37] In fact, storage of samples under nH_2 at liquid nitrogen temperatures before thawing and NMR detection led to one of the first reports of parahydrogen-induced

polarization (PHIP), as pH_2 enrichment was built up during sample storage.[4,43,44] Additionally, if there is an imperfect seal when filling the NMR tube, small amounts of oxygen could be introduced. This oxygen could then also act as a paramagnetic catalyst for the conversion of the spin isomers.[21]

Gamliel et al.[27] measured the conversion of pH_2 in NMR tubes (type of glass not specified), using an NMR method similar to that described above to determine the pH_2 fraction in the gas. They reported that no conversion of pH_2 occurred; however, they only monitored the samples for 20 min. Tom et al.[21] also measured the conversion of pH_2 in NMR tubes using NMR to monitor the pH_2 content. They reported that the back conversion to oH_2 at room temperature for a sample starting with $\approx 99.9\%$ pH_2 enrichment was 0.4% h^{-1} in tubes made from the same type of borosilicate glass as used here. Similarly, Feng et al.[15] monitored the conversion of pH_2 to oH_2 every 8 min for 64 h in an NMR tube. They found that the conversion profile followed an exponential function with a time constant of around 846 min. Hövener et al.[16] observed a similar profile in a borosilicate glass vial monitored over 41 h, again using NMR to determine the pH_2 fraction; they reported a similar time constant of around 820 min.

To determine whether conversion of pH_2 to oH_2 was occurring inside the NMR tubes used here, five different tubes were filled with H_2 from the pH_2 generator at 4 bar and then analyzed with Raman spectroscopy every 30 s for 40 min. The sampling was done in a similar manner to the at-line study described above, except that the NMR tube was left in the beam path of the laser between measurements, resulting in an in situ measurement of any conversion occurring inside the NMR tube. For three of the tubes it was found that almost no back-conversion occurred within 40 min. For instance, for one sample x_{pH_2} values were scattered around a mean of 40.5%, with a total range of about 1%, and a standard deviation of 0.3% (see Fig. S6). This indicates that good precision and repeatability can be achieved even with rapid sampling.

For two of the NMR tubes used, conversion from pH_2 to oH_2 occurred rapidly with a significant decrease in pH_2 fraction within 40 min. To investigate this further, these two tubes were refilled with fresh pH_2 to 4 bar and analyzed every 30 s for 3 h. The results are shown in Fig. 7, which shows that x_{pH_2} decreases very rapidly in both of these tubes, with complete conversion within 3 h and within 1 h for tubes 1 and 2, respectively. The two tubes that catalyzed the pH_2 to oH_2 conversion had very reproducible behavior. It was possible to fit an exponential to the decay of x_{pH_2} against time, where the fit had the same rate constant for each replicate experiment. The rate constant was 5.3×10^{-4} s^{-1} for tube 1 and 27.4×10^{-4} s^{-1} for tube 2. The reason for the vertical offset seen for tube 1 is that the tube was filled at different pH_2 generator running
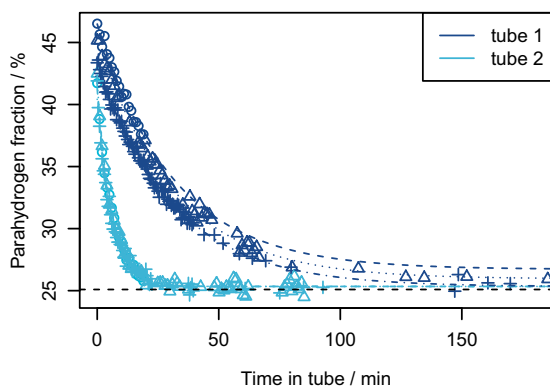
Figure 7. Plots of parahydrogen fraction (x_{pH_2}) against time for two NMR tubes found to accelerate the conversion of pH$_2$ to oH$_2$. x_{pH_2} was calculated from the in situ Raman spectrum of pH$_2$-enriched H$_2$ gas at 4 bar. Time zero was regarded as the time that the sample was filled from the pH$_2$ generator. Each color indicates a different tube and each symbol type is a different sample (refilled with fresh pH$_2$ each time) in the tube. The colored dashed and dotted lines show an exponential fit through the decay of x_{pH_2} against time (details in the main text). The black horizontal dashed line shows the equilibrium value x_{pH_2} at the measurement temperature.

times and so had slightly different starting values of x_{pH_2}. This suggests that these tubes were contaminated with some form of impurity that accelerates the conversion of pH$_2$ to oH$_2$.

These results show that by using in-situ Raman analysis it was possible to monitor a rapid reaction in the gas phase, which may have gone unnoticed with other analysis techniques. The results also highlight the need to check glassware used when working with pH$_2$-enriched gas, as many different types of impurities can promote the back conversion to oH$_2$.[2,5,37]

To determine the long-term stability of pH$_2$ in a non-contaminated tube, a fresh sample was analyzed every 20 min for a period of 18 h. This sample started with a x_{pH_2} of 43.0% and decayed with a linear rate of 0.08% h^{-1} to 41.6% (see Fig. S7). This confirms that pH$_2$ is very stable within the non-contaminated NMR tubes and thus any conversion will have a negligible impact on the level of x_{pH_2} for the measurement times used in the at-line and on-line monitoring discussed above ($\leq$50 s).

Conclusion

In this work, we have presented a rapid method to determine quantitatively the pH$_2$ fraction in H$_2$ gas using Raman spectroscopy. The Raman method has several advantages over other analytical techniques for determining pH$_2$ fraction, most notably that no calibration samples are required. Here, we used a NCO to acquire Raman spectra of H$_2$ gas at moderate pressures ($\leq$ 5 bar) from within standard NMR

tubes or a glass flow tube. This approach greatly simplifies the set-up and allows for much more rapid analysis compared to previous literature reports of using Raman spectroscopy to measure pH$_2$ fraction.[8,10,13,14,26]

The performance of an in-house built pH$_2$ generator was measured on-line by recording Raman spectra from a flow tube at the outlet of the generator. It was found that the generator required much longer than anticipated to reach steady state output (around 7 h). It was also found that increasing the flow rate of the gas within the generator reduces the enrichment achieved, presumably because of a reduction in residence time of the gas flowing in the generator. This result has important implications for hyperpolarization experiments requiring pH$_2$ such as SABRE, as the NMR signal enhancement achieved is proportional to the enrichment level of the pH$_2$ gas used.[4,11,15] The on-line monitoring method reported here could be used in the future to correlate the enhancement of the NMR signal by SABRE to the pH$_2$ fraction and to assess any changes to the pH$_2$ generator design.

The rapid nature of the analysis used here permitted Raman spectra to be acquired every 30 s, so that the fast interconversion of the spin isomers of hydrogen from an enriched composition back to the room temperature equilibrium fraction within contaminated NMR tubes could be followed in detail. This interconversion may have been unnoticed with other slower analytical methods. Our results reveal a clear challenge when working with what is predicted to be essentially identical NMR tubes. It is also vital to take note that many PHIP approaches use sealed NMR tubes and often monitor product formation over minutes to hours.[4,11,45,46] Significant care must therefore be taken in excluding sample preparation effects in such studies.

The results reported here for on-line and in-situ monitoring using commercially available hardware, represent close to a 500-fold increase in sensitivity compared to some previously reported work.[13] Improvement and customization of the experimental set-up, e.g., by the use of multiple optical passes, could be expected to further increase the signal. More generally, this work demonstrates that Raman spectroscopy can be used to quantify the pH$_2$ fraction in H$_2$ gas in a fast and convenient manner. This is important in many other applications which require pH$_2$, such as storage of H$_2$ for fuel.

Conflict of Interest

The authors report there are no conflicts of interest.

ORCID iD

Andrew J. Parrott http://orcid.org/0000-0002-4598-2736
Peter M. Richardson http://orcid.org/0000-0002-6631-2459
Olga Semenova http://orcid.org/0000-0002-5068-1460
Meghan E. Halse http://orcid.org/0000-0002-3605-5551
Alison Nordon http://orcid.org/0000-0001-6553-8993

References

1. A. Farkas. Orthohydrogen, Parahydrogen and Heavy Hydrogen. London: Cambridge University Press, 1935.
2. M. Matsumoto, J.H. Espenson. "Kinetics of the Interconversion of Parahydrogen and Orthohydrogen Catalyzed by Paramagnetic Complex Ions". J. Am. Chem. Soc. 2005. 127(32): 11447–11453.
3. R.A. Green, R.W. Adams, S.B. Duckett, R.W. Mewis, et al. "The Theory and Practice of Hyperpolarization in Magnetic Resonance Using Parahydrogen". Prog. Nucl. Magn. Reson. Spectrosc. 2012. 67: 1–48.
4. J. Natterer, J. Bargon. "Parahydrogen Induced Polarization". Prog. Nucl. Magn. Reson. Spectrosc. 1997. 31: 293–315.
5. G. Buntkowsky, B. Walaszek, A. Adamczyk, Y. Xu, et al. Mechanism of Nuclear Spin Initiated Para-H_2 to Ortho-H_2 Conversion". Phys. Chem. Chem. Phys. 2006. 8(16): 1929–1935.
6. J.L. Sloop. Liquid Hydrogen as a Propulsion Fuel, 1945–1959. NASA History Series. Scotts Valley, CA: CreateSpace Independent Publishing Platform, 2016. https://history.nasa.gov/SP-4404/app-a3.htm.
7. W.F. Baade, U.N. Parekh, V.S. Raman. "Hydrogen". Kirk-Othmer Encyclopedia of Chemical Technology. Hboken, NJ: John Wiley and Sons, 2000.
8. G. Petitpas, S.M. Aceves, M.J. Matthews, J.R. Smith. "Para-H_2 to Ortho-H_2 Conversion in a Full-Scale Automotive Cryogenic Pressurized Hydrogen Storage up to 345 Bar". Int. J. Hydrogen. Energy. 2014. 39(12): 6533–6547.
9. S. Tam, M.E. Fajardo. "Ortho/Para Hydrogen Converter for Rapid Deposition Matrix Isolation Spectroscopy". Rev. Sci. Instrum. 1999. 70(4): 1926–1932.
10. K. Sundararajan, K. Sankaran, N. Ramanathan, R. Gopi. "Production and Characterization of Para-Hydrogen Gas for Matrix Isolation Infrared Spectroscopy". J. Mol. Struct. 2016. 1117: 181–191.
11. L.T. Kuhn, editor. Hyperpolarization Methods in NMR Spectroscopy. Number 338 in Topics in Current Chemistry. Heidelberg: Springer, 2013.
12. S.B. Duckett, R.E. Mewis. "Application of Parahydrogen Induced Polarization Techniques in NMR Spectroscopy and Imaging". Acc. Chem. Res. 2012. 45(8): 1247–1257.
13. L.M. Sutherland, J.N. Knudson, M. Mocko, R.M. Renneke. "Practical In-Situ Determination of Ortho-Para Hydrogen Ratios Via Fiber-Optic Based Raman Spectroscopy". Nucl. Instrum. Methods Phys. Res., Sect. A. 2016. 810: 182–185.
14. M. Teshigawara, M. Harada, H. Tatsumoto, T. Aso, et al. "Experimental Verification of Equilibrium Para-Hydrogen Levels in Hydrogen Moderators Irradiated by Spallation Neutrons at J-PARC". Nucl. Instrum. Methods Phys. Res., Sect. B. 2016. 368: 66–70.
15. B. Feng, A.M. Coffey, R.D. Colon, E.Y. Chekmenev, et al. "A Pulsed Injection Parahydrogen Generator and Techniques for Quantifying Enrichment". J. Magn. Reson. 2012. 214: 258–262.
16. J.B. Hövener, S. Bär, J. Leupold, K. Jenne, et al. "A Continuous-Flow, High-Throughput, High-Pressure Parahydrogen Converter for Hyperpolarization in a Clinical Setting". NMR Biomed. 2013. 26(2): 124–131.
17. Bruker. "Parahydrogen Generator". https://www.bruker.com/products/mr/nmr/accessories/hyperpolarization/parahydrogen-generator/overview.html [accessed Jul 27 2018].
18. M.E. Halse. "Perspectives for Hyperpolarisation in Compact NMR". TrAC, Trends Anal. Chem. 2016. 83: 76–83.
19. P.M. Richardson, S. Jackson, A.J. Parrott, A. Nordon, et al. "A Simple Hand-Held Magnet Array for Efficient and Reproducible SABRE Hyperpolarisation Using Manual Sample Shaking". Magn. Reson. Chem. 2018. 56: 641–650.
20. P.M. Richardson, A.J. Parrott, O. Semenova, A. Nordon, et al. "SABRE Hyperpolarization Enables High-Sensitivity ^{1}H and ^{13}C Benchtop NMR Spectroscopy". Analyst. 2018. 143: 3442–3450.
21. B.A. Tom, S. Bhasker, Y. Miyamoto, T. Momose, et al. "Producing and Quantifying Enriched Para-H_2". Rev. Sci. Instrum. 2009. 80(1): 016108.
22. N. Sakoda, K. Shindo, K. Shinzato, M. Kohno, et al. "Review of the Thermodynamic Properties of Hydrogen Based on Existing Equations of State". Int. J. Thermophys. 2010. 31(2): 276–296.
23. J.W. Leachman, R.T. Jacobsen, S.G. Penoncello, E.W. Lemmon. "Fundamental Equations of State for Parahydrogen, Normal Hydrogen, and Orthohydrogen". J. Phys. Chem. Ref. Data. 2009. 38(3): 721–748.
24. T.W. Bradshaw, J.O.W. Norris. "Observations on the Use of a Thermal Conductivity Cell to Measure the Para Hydrogen Concentration in a Mixture of Para and Ortho Hydrogen Gas". Rev. Sci. Instrum. 1987. 58(1): 83–85.
25. P.A. Fleury, J.P. McTague. "Molecular Interactions in the Condensed Phases of Ortho-Para Hydrogen Mixtures". Phys. Rev. 1975. 12(1): 317–326.
26. M.J. Matthews, G. Petitpas, S.M. Aceves. "A Study of Spin Isomer Conversion Kinetics in Supercritical Fluid Hydrogen for Cryogenic Fuel Storage Technologies". Appl. Phys. Lett. 2011. 99(8): 1–4.
27. A. Gamliel, H. Allouche-Arnon, R. Nalbandian, C.M. Barzilay, et al. "An Apparatus for Production of Isotopically and Spin-Enriched Hydrogen for Induced Polarization Studies". Appl. Magn. Reson. 2010. 39(4): 329–345.
28. R.E. Mewis, K.D. Atkinson, M.J. Cowley, S.B. Duckett, et al. "Probing Signal Amplification by Reversible Exchange Using an NMR Flow System". Magn. Reson. Chem. 2014. 52(February): 358–369.
29. L.S. Lloyd, R.W. Adams, M. Bernstein, S. Coombes, et al. "Utilization of SABRE Derived Hyperpolarization to Detect Low Concentration Analytes via 1D- and 2D-NMR Methods". J. Am. Chem. Soc. 2012. 134: 12904–12907.
30. R Core Team. R: A Language and Environment for Statistical Computing. Vienna, Austria: R Foundation for Statistical Computing, 2017. https://www.R-project.org/.
31. C. Beleites, V. Sergo. hyperSpec: a package to handle hyperspectral data sets in R, 2016. http://hyperspec.r-forge.r-project.org.
32. K.H. Liland, B.H. Mevik. baseline: Baseline Correction of Spectra. Vienna, Austria: R Foundation for Statistical Computing, 2015. https://CRAN.R-project.org/package=baseline.
33. D.V. Petrov, I.I. Matrosov. "Raman Gas Analyzer (RGA): Natural Gas Measurements". Appl. Spectrosc. 2016. 70(10): 1770–1776.
34. D.V. Petrov, I.I. Matrosov. "Pressure Dependence of the Raman Signal Intensity in High-Pressure Gases". J. Raman. Spectrosc. 2017. 48: 474–478.
35. J. Kiefer. "Recent Advances in the Characterization of Gaseous and Liquid Fuels by Vibrational Spectroscopy". Energies. 2015. 8: 3165–3197.

36. S.C. Eichmann, M. Weschta, J. Kiefer, T. Seeger, et al. "Characterization of a Fast Gas Analyzer Based on Raman Scattering for the Analysis of Synthesis Gas". Rev. Sci. Instrum. 2010. 81(12): 125104.

37. E. Ilisca. "Ortho-Para Conversion of Hydrogen Molecules Physisorbed on Surfaces". Prog. Surf. Sci. 1992. 41: 217–335.

38. P.W. Atkins, J. de Paula. Atkins' Physical Chemistry. Oxford, UK: Oxford University Press, 2010. 9th ed.

39. J.L. Hunt, J.D. Poll, L. Wolniewicz. "Ab Initio Calculation of Properties of the Neutral Diatomic Hydrogen Molecules H_2, HD, D_2, HT, DT, and T_2. Can. J. Phys. 1984. 62: 1719–1723.

40. S.B. Duckett, C.J. Sleigh. "Applications of the Parahydrogen Phenomenon: A Chemical Perspective". Prog. Nucl. Magn. Reson. Spectrosc. 1999. 34(1): 71–92.

41. I. Reile, R.L.E.G. Aspers, J.M. Tyburn, J.G. Kempf, et al. "DOSY Analysis of Micromolar Analytes: Resolving Dilute Mixtures by SABRE Hyperpolarization". Angew. Chem. Int. Ed. 2017. 56: 9174–9177.

42. E.W. Lemmon, M.O. McLinden, D.G. Friend. "Thermophysical Properties of Fluid Systems". In: NIST Chemistry WebBook, NIST Standard Reference Database Number 69. Gaithersburg, MD: National Institute of Standards and Technology, 2018.

43. R. Eisenberg. "Parahydrogen-Induced Polarization: A New Spin on Reactions with H_2". Acc. Chem. Res. 1991. 24(4): 110–116.

44. T.C. Eisenschmid, R.U. Kirss, P.P. Deutsch, S.I. Hommeltoft, et al. "Para Hydrogen Induced Polarization in Hydrogenation Reactions". J. Am. Chem. Soc. 1987. 109(26): 8089–8091.

45. D. Blazina, S.B. Duckett, J.P. Dunne, C. Godard. "Applications of the Parahydrogen Phenomenon in Inorganic Chemistry". Dalton Trans. 2004. 17): 2601–2609.

46. S.B. Duckett, N.J. Wood. "Parahydrogen-Based NMR Methods as a Mechanistic Probe in Inorganic Chemistry". Coord. Chem. Rev. 2008. 252(21–22): 2278–2291.